

Construction of continuous collective energy landscapes for large amplitude nuclear many-body problems

Paul Carpentier,^{1,2} Nathalie Pillet,^{1,2,*} Denis Lacroix,^{3,†} Noël Dubray,^{1,2} and David Regnier^{1,2}

¹CEA, DAM, DIF, 91297 Arpajon, France

²Université Paris-Saclay, CEA, Laboratoire Matière en Conditions Extrêmes, 91680 Bruyères-le-Châtel, France

³Université Paris-Saclay, CNRS/IN2P3, IJCLab, 91405 Orsay, France

(Dated: May 29, 2024)

Several protocols are proposed to build continuous energy surfaces of many-body quantum systems, regarding both energy and states. The standard variational principle is augmented with constraints on state overlap, ensuring arbitrary precision on continuity. As an illustration, the lowest energy and excited state paths relevant for the ²⁴⁰Pu asymmetric fission are studied. The scission is clearly signed, with a neutron excess in the neck, the ultimate glue before its rupture. Our approach can potentially connect any couple of Hilbert space states, which opens up new horizons for various applications.

Keywords: Variational principle, Mean-Field theory, Energy landscapes

Energy landscapes in a physical problem provide crucial information on the static and/or dynamic properties of the system under interest. In complex quantum systems, like interacting particles, due to the factorial growing of the number of degrees of freedom (DOFs) with the number of particles, such potential energy surfaces (PESs) can only be obtained in a rather low dimension, with a few selected, physically guided, collective DOFs. Typically, in atomic nuclei, these DOFs reflect the deformation of the quantum nuclear droplet.

A recurrent difficulty observed in complex systems while calculating PESs is the occurrence of many discontinuities [1–10] either in the energies or in the overlap between adjacent states, or in both. Various origins of these discontinuities have been identified. For instance, when building up PESs from a variational principle, one might suddenly jump from one state to a very different state by spontaneous symmetry breaking. Even without any discontinuity in energy, the PES might connect two different energy landscapes that could not be dissociated when focusing solely on a few DOFs. This leads to the difficulty that even an infinitesimal change in the selected DOFs can lead to orthogonality between many-body states.

These difficulties are fingerprints of the complexity of many-body systems, whose PESs should be built as a multidimensional problem with a large set of dimensions and whose evolution might reflect the existence of many local, almost degenerated minima. Having discontinuities and/or jumps between completely different states is a severe difficulty when one tries to obtain a fully quantum description of the dynamical properties of a many-body system, for instance when performing the evolution of the collective wave function, as is done in the time-dependent generator coordinate method [11–15]. Also,

from first-principle arguments based on the continuity equation, an evolving quantum system should have a continuous evolution of its local density and, in no way, can jump instantaneously from one shape to another.

A possible solution to these problems is to increase the number of relevant DOFs with the limitation that the solution of a Schrödinger equation can hardly be found in more than three dimensions. Another solution is to find a practical way to get around the problem while keeping the collective space dimension tractable for further post-processing. Solving the latter problem is a milestone for the future applicability of most of the adiabatic methods, for instance applied to the problem of fission [16, 17]. Not surprisingly, several attempts to solve this problem in nuclear physics have been made over the years [18–20].

Lastly, we would like to stress that the situation becomes even more critical when implementing non-adiabatic effects by including PESs associated not only with lowest energy states but also excited states [21–25]. This problem was the original motivation of the present work. The solution we give here can be implemented in state-of-the-art nuclear density functional models and solve the problem of discontinuities for various low-lying states, including the lowest energy ones, without increasing the dimension of the collective space.

Intending to build a smooth and continuous energy landscape both in energy and trial wave functions, we firstly reduced the problem to its simplest form: *Given two many-body states A and B , is it possible to find a continuous path between them while minimizing the total binding energy using specific variational techniques?* This problem transforms into finding a set of states that will form a path from A to B , where we can gradually decrease the kernel to A and increase the kernel to B . The measure of the kernel between the states A and B will be made using the metric $d(A, B) = \text{Tr}(\hat{D}_A \hat{D}_B)$ where $\hat{D}_{A/B}$ are the density matrices of the two states. In this process, some states (A) will be repulsive since we want to escape from them, while others (B) will have an attractive role. Those states will be referred to as repulsors

*Electronic address: nathalie.pillet@cea.fr

†Electronic address: lacroix@ijclab.in2p3.fr

or attractors, respectively. This simple example can be extended to a more general situation. Assume that we already have a set of states $\{C_k\}_{k=1,\dots,K}$, some of these states being attractors and some repulsors, and we want to build a new state, using for instance a variational approach to minimize the total energy. This problem can be replaced by a modified variational principle, adding a set of Lagrange multipliers to control the kernel between the new state and the different states C_k . The strategy we propose is to apply the following generalized variational principle:

$$\delta \text{Tr} \left\{ \hat{D} \left(\hat{H}_c - \sum_k \beta_k [\hat{D}_k - d_k] - E \right) \right\} = 0, \quad (1)$$

where \hat{H}_c is the Hamiltonian \hat{H} augmented with some constraints:

$$\hat{H}_c \equiv \hat{H} - \sum_{\alpha} \lambda_{\alpha} [\hat{Q}_{\alpha} - q_{\alpha}]. \quad (2)$$

$\{\hat{Q}_{\alpha}\}_{\alpha=1,d}$ is a set of constraints, for instance the shape, the particle number... of the quantum droplet. The novel aspect here is the addition of a new set of constraints on the system kernel with the configurations, through the constraint of $\text{Tr}(\hat{D}\hat{D}_k)$. Here, $\hat{D}_k \equiv |C_k\rangle\langle C_k|$ are new operators added to control the kernel of \hat{D} with the predefined configurations $|C_k\rangle$. The Lagrange multipliers are adjusted such that, at the minimum, we have:

$$\langle \hat{Q}_{\alpha} \rangle = q_{\alpha}, \quad \langle \hat{D}_k \rangle = \text{Tr}(\hat{D}\hat{D}_k) = d_k, \quad (3)$$

where we use the short-hand notations $\langle \cdot \rangle = \text{Tr}(\hat{D}\cdot)$. Although this method can be used in more general situations like mixed states, we will only consider here the case of pure states for which $\hat{D} = |\Psi\rangle\langle\Psi|$. We note that $\langle \hat{D}_k \rangle$ is nothing but the kernel of the system with the configurations $\{|C_k\rangle\}$. Eventually, d_k can be set to 0 (full repulsor) or 1 (full attractor).

We mention that the *Deflation method*, known as a general method to solve eigenvalue problems [26] was employed recently in quantum chemistry [27] and used to calculate excited states for the nuclear many-body problem [28, 29], is a special case of the more general method we develop here. The variational principle (1) turns out to be a versatile tool that can solve the various difficulties in constructing smooth PESs relevant to the description of atomic nuclei. Examples of the approach to PESs relevant to nuclear physics with a focus on the fission process are given below. Noteworthy, all the applications below make connection between quasiparticle (QP) vacua for which the Thouless theorem [30, 31] simplifies the variation of the constraints based on the overlaps. Indeed, starting from a QP state $|\Psi_0\rangle$ associated with a set of quasiparticle operators $\{\beta_{\lambda}^{\dagger}\}_{\lambda=1,\Omega}$, any surrounding QP state can be parameterized as $|\Psi(\mathbf{Z})\rangle = e^{-\sum_{\lambda\lambda'} Z_{\lambda\lambda'} \beta_{\lambda}^{\dagger} \beta_{\lambda'}^{\dagger}} |\Psi_0\rangle$. Then, the state

variation reduces to the variations of the \mathbf{Z} matrix elements and of the overlap $\langle\Psi(\mathbf{Z})|C\rangle$, where $|C\rangle$ is a fixed QP state:

$$\partial_{Z_{\lambda\lambda'}}^* \langle\Psi(\mathbf{Z})|C\rangle \Big|_{\mathbf{Z}=0} = \langle\Psi_0|\beta_{\lambda}\beta_{\lambda'}|C\rangle, \quad (4)$$

which can be evaluated numerically using standard techniques for quasiparticle states, as shown in [32].

Three protocols based on the minimization of Eq.(1) are developed below. The first one is called hereafter *Link method*. Its goal is to link/connect two Hartree-Fock-Bogolyubov (HFB) states ($|A\rangle$ and $|B\rangle$) through a set $|C_i\rangle$ of HFB states iteratively, so that adjacent states present a given kernel value. Ultimately, the set of states $\{|C_i\rangle\}_{i=0,\dots,M}$ forms a continuous path in the many-body space from $|A\rangle$ to $|B\rangle$. The key parameter to generate the path is a constant $0 < d < 1$ that fixes the squared overlap $d = |\langle C_i|C_{i-1}\rangle|^2$. The initial state is fixed so that $|C_0\rangle = |A\rangle$. The variational principle is minimized to seek for a new state $|C_1\rangle$ with the constraint $|\langle C_0|C_1\rangle|^2 = d$ and $|\langle C_1|B\rangle|^2$ is maximized. Note that eventual constraints on multipole moments are not imposed, allowing the state to explore various shapes. The center of mass position and particle numbers are constrained during the minimization. At the end of this step, a state $|C_1\rangle$ is obtained. The procedure is then iterated. At the i -th iteration, starting from the state $|C_i\rangle$, a new state $|C_{i+1}\rangle$ is generated, imposing the overlap with the previous state to be d while maximizing the overlap with the state $|B\rangle$. The iteration stops when the overlap between the last generated state and $|B\rangle$ is greater or equal to d . This method allows us to obtain low-energy PESs that are, in practice, very close to the adiabatic limit usually employed in nuclear physics while being continuous both in energy and overlap. In practice, one can choose a value $|d-1| \leq \epsilon$, requiring $\epsilon \ll 1$ to give direct control of the continuity in the overlap of adjacent states along the path. Decreasing ϵ leads to an increase in the number of trial states that are used to build the PESs.

Even if the *Link method* works well to connect two HFB states, the requirement of having both a starting and a final states is no longer fulfilled when it comes to describing situations wherein final configurations are not known *a priori*, as for the scission process. The *Drop method* has been developed to tackle this issue. It creates an adiabatic and continuous path from a starting configuration, only following an energy descent. This method is "goal-free" and thus enables us to adequately describe processes such as the scission one. It starts with an HFB state $|A\rangle = |C_0\rangle$ and finds the state $|C_1\rangle$ minimizing the energy while ensuring $|\langle C_0|C_1\rangle|^2 = d$. This procedure is then iterated from $|C_i\rangle$ to find $|C_{i+1}\rangle$. It stops after a given number of iterations or whenever the energy of $|C_{i+1}\rangle$ exceeds that of $|C_i\rangle$. While the *Link method* allows to obtain continuous low-energy PESs from discontinuous ones, staying very close to the adiabatic limit usually employed in nuclear physics, the *Drop method*, where the

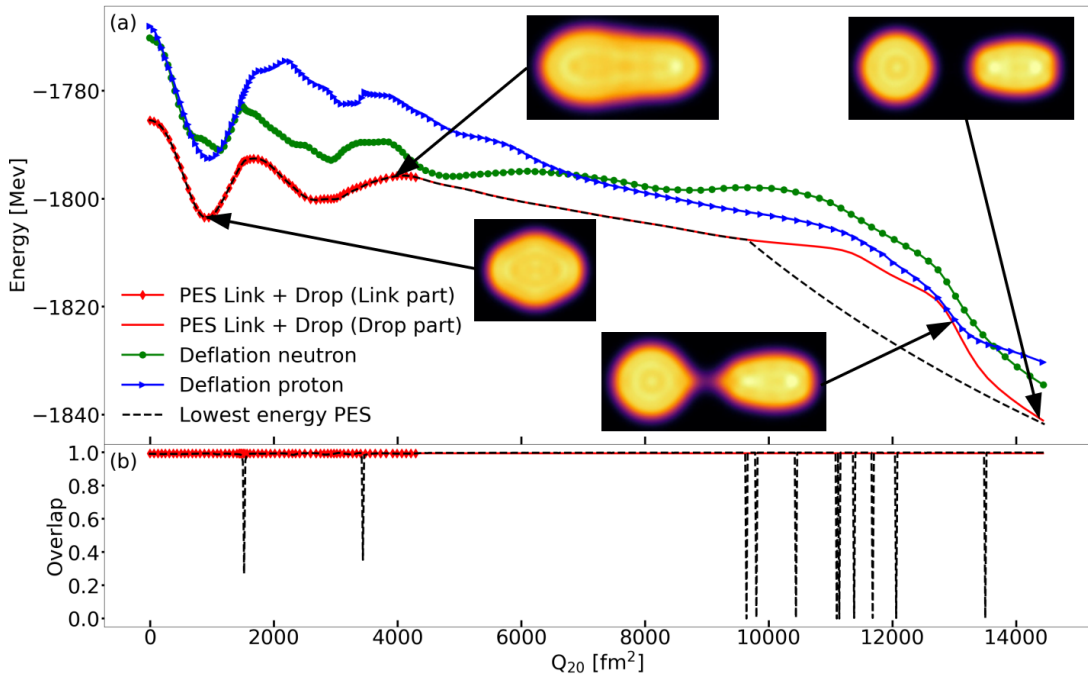


FIG. 1: Panel (a): some PESs (red, green, and blue curves) obtained with the different variational protocols based on Eq.(1). They have been calculated for ^{240}Pu as a function of the mass quadrupole moment (Q_{20}), with a continuity $d = 0.990$. For comparison, the black dashed line corresponds to the solutions obtained with conventional minimization techniques (adiabatic limit). All PESs present a continuous evolution of the total binding energy. Note that four times more calculations have been done than those represented here by symbols for clarity reasons. The entire red solid line has been obtained using the *Link* and *Drop* methods. More precisely, solutions corresponding to red diamonds are based on the *Link* method, while the solutions forming the continuous red curve result from the *Drop* method. After following the adiabatic path, the *Drop* method continuously connects to the usual Coulomb PES at $\langle Q_{20} \rangle > 14.10^3 \text{ fm}^2$. The different insets show spatial and local 1-body total nuclear density slices for some striking states. The *Deflation* method has been used to produce a neutron (proton) excited PES in green (blue), imposing orthogonality with the corresponding red HFB solution while ensuring the same d value. Note that we have calculated ten excited states with the *Deflation* method and have obtained very stable results (not shown here). Panel (b): Overlap between each state and its adjacent state for the red and black curves. We can see some isolated single low values of the overlap for the black curve, corresponding to discontinuities as discussed in the introduction. The *Link+Drop* method allows a constant high value of the overlap shown here for the red curve.

constraint on the final target is relaxed, generates paths that wouldn't have been possible to describe without it.

The *Drop* method is efficient on the descent to scission when usual approaches using multipole moments struggle to describe the nucleus continuously just before scission and fail most of the time to obtain reliably separated fragments. Those difficulties are systematically observed in such studies, and tentative solutions have been proposed using additional geometrical constraints [33–35], but without controlling the continuity of the states. Continuously crossing the scission is crucial to make contact with experimental observations since, after separation, daughter nuclei essentially only encounter the Coulomb boost with eventual in-flight post-equilibrium emissions. Methods to extract the PES were also proposed based on the nuclear Time-Dependent Density Functional Theory (TDDFT). TDDFT has the advantage of ensuring continuity in the trial state vector and can also go through the scission region. However, specific methods should

be developed to separate static and dynamical effects in the PES [36, 37]. Additionally, the path followed in TDDFT is sometimes too diabatic, preventing the description from the saddle point [39, 40], and explores restricted regions in the collective space [41].

PESs obtained by combining the *Link* and *Drop* methods are shown in Fig.1, panel (a). The D1S Gogny interaction has been used [11, 12, 42–44] as well as a new HFB solver whose solutions are expanded on an axial two-center harmonic oscillator basis allowing the breaking of parity symmetry [45]. The standard technique to generate adiabatic PESs (black dashed line) leads to a continuous energy evolution but significant kernel jumps in adjacent state vectors obtained by energy minimization. For instance, the second sudden jump observed in the overlap shown in Fig.1, panel (b), signs the quantum phase transition from symmetric to asymmetric nuclear shapes due to the spontaneous breaking of the parity symmetry, the first discontinuity at large quadrupole mo-

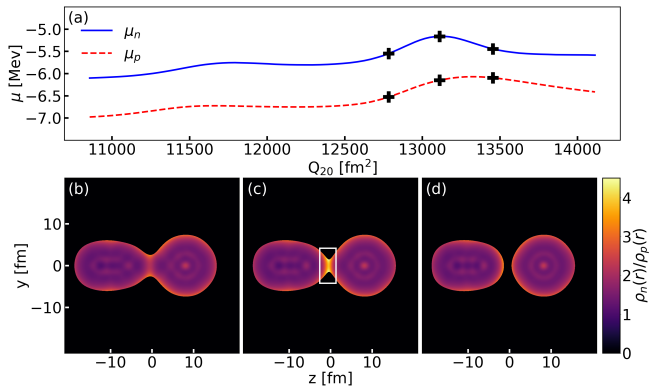


FIG. 2: Panel (a): Evolution of the neutron (blue line) and proton (red dashed line) chemical potentials $\mu_{n,p}$ along the *Link+Drop* path shown in Fig.1. Panels (b-d): Ratio $\rho_n(\mathbf{r})/\rho_p(\mathbf{r})$ between neutron and proton 1-body local densities for a total density $\rho(\mathbf{r})$ exceeding the threshold value $5.10^{-3} \text{ fm}^{-3}$. The (b) to (d) states are indicated in panel (a) by black crosses. The white box in panel (c) delimits the region where the neutron-to-proton fraction is maximally enhanced.

ment Q_{20} signs the Coulomb-fission valleys crossing, and the following ones highlight the complex structure of the Coulomb valley. The *Link method* allows the generation of a PES very close to the adiabatic one while ensuring an overlap between adjacent states that is precisely controlled using a high kernel value $d = 0.990$. Noteworthy, using the *Drop method* at a large quadrupole moment Q_{20} also leads to a continuous overlap while connecting without problem the PESs to the Coulomb energy surface. As far as we know, this is the first-ever continuous connection of the fission valley to the Coulomb valley using such fine quantitative control of the overlap between adjacent states.

The possibility of accessing the full path to dissociation in ^{240}Pu allowed us to uncover an interesting phenomenon illustrated in Fig 2, panel (a), which shows the neutron and proton chemical potentials, μ_n and μ_p , along the *Link+Drop* path. As the fragments separate, we see that neutrons are less bound than protons with a sudden increase of $\mu_{n,p}$ that signs the neck rupture. Just before the rupture, an excess of neutrons appears in the neck. This is illustrated in Fig.2, panels (b-d). Here, the ratio between the local neutron and proton 1-body densities reaches values three times larger than the ratio $N/Z = 1.55$. This enrichment is due to a single neutron quasiparticle state strongly localized at the neck before the scission that serves as the ultimate glue between the two daughter nuclei before the separation. This phenomenon looks very similar to the electrons that bind molecules or the generalized version of the Ikeda diagram introduced for clustering classification in neutron-rich nuclei [54], excepted that for fission, this configuration is an intermediate step towards the final separation. Finally, the mean total kinetic energy, estimated by simply

accounting for the Coulomb re-acceleration at the neck rupture assumed to occur at the maximum of μ_n (second cross in Fig.2, panel (a)), is found to be 175.4 MeV. This value is very close to the 177.7 MeV measured experimentally [50, 51].

A third protocol based on Eq.(1), called hereafter *Deflation*, is proposed to build continuous PESs for excited states. Provided that we have already constructed a set of states $\{|C_k\rangle\}_{k=1,\dots,M}$ associated with the lowest energy landscape with the *Link* and *Drop methods*, we then use these states as pure repulsors to build the first excited state PES. As an example relevant for fission studies, for a neutron (proton) excitation, Eq.(1) is solved imposing that the neutron (proton) part of the HFB reference state is orthogonal to the neutron $|C_i\rangle$ state one ($d_i \simeq 0$) while the proton (neutron) parts of both states are required to be equal ($d_{i'} \simeq 1$). Having the first excited state PES, the second excited state one is obtained by imposing the simultaneous orthogonality to the lowest energy and the first excited PESs, and so on and so forth. Two examples of such excited state PESs, obtained by imposing orthogonality either with the neutron or proton lowest energy wave functions, are shown in Fig.1, panel (a). In both cases, a near-perfect orthogonality with the lowest energy states and a near-perfect continuity between adjacent excited states are reached. The method has been tested to build up to ten successive excited states of this type without specific difficulties. More general excited states can also be generated by the *Deflation method*.

By adding constraints on overlaps when building collective PESs for many-body self-bound systems, we propose a set of versatile protocols based on the variational principle (1) that ensures continuity both in energy and in the states themselves for a set of low-lying states, without increasing the number of DOFs. While PESs with continuous energy are standard, the control of continuity in states has been missing so far. It will open opportunities in applications that were difficult or even impossible until now. To quote some of them in the nuclear physics context, one can mention the possibility of performing time-dependent configuration mixing using overlap kernels without approximation. The availability of excited state PESs will also allow the inclusion of non-adiabatic effects during the evolution and the onset of internal excitation [21, 22]. This is one of the paths to describe dissipative effects and quantum collective fluctuations on the same footing in a common framework. In a completely different topic, since the method also allows to connect various configurations in the Hilbert space, one can use it to address the problem of clustering in atomic nuclei and connect in a continuous way normal configurations with configurations presenting clusters, as well as cluster emission [54–60].

Acknowledgement: NP and PC would like to thank L. Robledo, R. Bernard and W. Younes for valuable discussions. DL thanks Y. Beaujeault-Taudière for the discus-

sions on the *Deflation method* at the early stage of this work. DL acknowledge the support of the IN2P3-AIQI

project.

-
- [1] A. Zaitsevskii and J.-P. Malrieu, The discontinuities of state-average MCSCF potential surfaces, *Chem. Phys. Lett.* **228**, 458 (1994).
- [2] H. B. Schlegel, Exploring potential energy surfaces for chemical reactions: An overview of some practical methods, *Journal of Computational Chemistry* **24**, 1514 (2003).
- [3] N. J. Russ and T. D. Crawford, Potential energy surface discontinuities in local correlation methods, *J. Chem. Phys.* **121**, 691 (2004).
- [4] C. Evenhuis and T. J. Martínez, A scheme to interpolate potential energy surfaces and derivative coupling vectors without performing a global diabaticization, *J. Chem. Phys.* **135**, 224110 (2011).
- [5] N. Dubray and D. Regnier, Numerical search of discontinuities in self-consistent potential energy surfaces, *Comput. Phys. Commun.* **183**, 2035 (2012).
- [6] D. Regnier, N. Dubray, and N. Schunck, From asymmetric to symmetric fission in the fermium isotopes within the time-dependent generator-coordinate-method formalism, *Phys. Rev. C* **99**, 024611 (2019).
- [7] J.A. Berger, Pierre-Francois Loos and Pina Romaniello, Potential Energy Surfaces without Unphysical Discontinuities: The Coulomb Hole Plus Screened Exchange Approach, *J. Chem. Theory Comput.* **17**, 191 (2021).
- [8] A.S. Hansen, E. Aurbakken and T.B. Pedersen, Smooth potential energy surfaces in fragmentation-based local correlation methods for periodic systems, *Molecular Physics*, 119:9 (2021).
- [9] S. Manzhos and T. J. Carrington, Neural Network Potential Energy Surfaces for Small Molecules and Reactions, *Chem. Rev.* **121**, 10187 (2021).
- [10] A. Zdeb, M. Warda, and L. M. Robledo, Description of the multidimensional potential-energy surface in fission of ^{252}Cf and ^{258}No , *Phys. Rev. C* **104**, 014610 (2021).
- [11] J.F. Berger, M. Girod, D. Gogny, Constrained Hartree-Fock and beyond, *Nucl. Phys. A* **502**, 85 (1989).
- [12] J.F. Berger, M. Girod, D. Gogny, Time-dependent quantum collective dynamics applied to nuclear fission, *Comput. Phys. Commun.* **63**, 365 (1991)
- [13] DL. Hill and J.A. Wheeler, Nuclear constitution and the interpretation of fission phenomena, *Phys. Rev.* **89**, 1102 (1953).
- [14] J.J. Griffin and J.A. Wheeler, Collective motions in nuclei by the method of generator coordinates, *Phys. Rev.* **108**, 311 (1957).
- [15] H. Goutte, J. F. Berger, P. Casoli, and D. Gogny, Microscopic approach of fission dynamics applied to fragment kinetic energy and mass distributions in ^{238}U *Phys. Rev. C* **71**, 024316 (2005)
- [16] N. Schunck and L. M. Robledo, Microscopic theory of nuclear fission: A review, *Rep. Prog. Phys.* **79**, 116301 (2016).
- [17] N. Schunck and D. Regnier, Theory of Nuclear Fission, *Prog. Part. Nucl. Phys.* **125**, 103963 (2022)
- [18] N.-W. T. Lau, R. N. Bernard, and C. Simenel, Smoothing of one- and two-dimensional discontinuities in potential energy surfaces, *Phys. Rev. C* **105**, 034617 (2022)
- [19] Raphaël-David Lasserri, David Regnier, Mikael Frosini, Marc Verriere, Nicolas Schunck, Generative deep-learning reveals collective variables of Fermionic systems, arXiv:2306.08348, accepted for publication in *Phys. Rev. C*.
- [20] G. Scamps and Y. Hashimoto, Density-constrained time-dependent Hartree-Fock-Bogoliubov method, *Phys. Rev. C* **100**, 024623 (2019).
- [21] K. Dietrich, J.-J. Niez, and J.-F. Berger, Microscopic approach to nuclear fission, *Int. J. Mod. Phys. E* **19**, 04, 521 (2010).
- [22] R. Bernard, H. Goutte, D. Gogny, W. Younes, Microscopic and nonadiabatic Schrödinger equation derived from the generator coordinate method based on zero- and two-quasiparticle states, *Phys. Rev. C* **84**, 044308 (2011).
- [23] W. Younes, D. M. Gogny, and J.-F. Berger, Microscopic Theory of Fission Dynamics Based on the Generator Coordinate Method, series of Lecture Notes in Physics, Springer International Publishing, 2019.
- [24] G. F. Bertsch and K. Hagino, Generator coordinate method for transition-state dynamics in nuclear fission, *Phys. Rev. C* **105**, 034618 (2022).
- [25] J. Zhao, T. Nikšić, and D. Vretenar, Time-dependent generator coordinate method study of fission: Dissipation effects, *Phys. Rev. C* **105**, 054604 (2022).
- [26] Y. Saad, Iterative methods for sparse linear systems, Society for Industrial and Applied Mathematics, 2003.
- [27] Oscar Higgott and Daochen Wang and Stephen Brierley, Variational Quantum Computation of Excited States, *Quantum* **3**, 156, (2019).
- [28] Michele Grossi, Oriel Kiss, Francesco De Luca, Carlo Zollo, Ian Gremese, and Antonio Mandarino, Finite-size criticality in fully connected spin models on superconducting quantum hardware, *Phys. Rev. E* **107**, 024113 (2023).
- [29] Yann Beaujeault-Taudière and Denis Lacroix, Solving the Lipkin model using quantum computers with two qubits only with a hybrid quantum-classical technique based on the Generator Coordinate Method, *Phys. Rev. C* **109**, 024327 (2024).
- [30] P. Ring and P. Schuck, The Nuclear Many-Body Problem (Springer-Verlag, New-York, 1980).
- [31] J. P. Blaizot and G. Ripka, Quantum Theory of Finite Systems (MIT Press, Cambridge, 1986).
- [32] L. M. Robledo, Operator overlaps in harmonic oscillator bases with different oscillator lengths, *Phys. Rev. C* **105**, 044317 (2022).
- [33] W. Younes, D. Gogny, Nuclear Scission and Quantum Localization, *Phys. Rev. Lett.* **107**, 13250 (2011).
- [34] M. Warda, A. Staszczak, and W. Nazarewicz, Fission modes of mercury isotopes, *Phys. Rev. C* **86**, 024601 (2012).
- [35] P. Marević, N. Schunck, J. Randrup, and R. Vogt, Angular Momentum of Fission Fragments from Microscopic Theory, *Phys. Rev. C* **104**, 021601 (2021).
- [36] A. S. Umar, V. E. Oberacker, J. A. Maruhn and P-G

- Reinhard, Microscopic description of nuclear fission dynamics, *J. Phys. G: Nucl. Part. Phys.* **37** 064037 (2010).
- [37] Yusuke Tanimura, Denis Lacroix, and Guillaume Scamps, Collective aspects deduced from time-dependent microscopic mean-field with pairing: Application to the fission process, *Phys. Rev. C* **92**, 034601 (2015).
- [38] Liang Tong and Shiwei Yan, Microscopic investigations into fission dynamics beyond the saddle point *Phys. Rev. C* **106**, 044611 (2022).
- [39] Philip Goddard, Paul Stevenson, and Arnau Rios, Fission dynamics within time-dependent Hartree-Fock: Deformation-induced fission, *Phys. Rev. C* **92**, 054610 (2015).
- [40] Philip Goddard, Paul Stevenson, and Arnau Rios, Fission dynamics within time-dependent Hartree-Fock. II. Boost-induced fission, *Phys. Rev. C* **93**, 014620 (2016).
- [41] Aurel Bulgac, Shi Jin, Kenneth J. Roche, Nicolas Schunck, and Ionel Stetcu, Fission dynamics of ^{240}Pu from saddle to scission and beyond *Phys. Rev. C* **100**, 034615 (2019).
- [42] J. Dechargé and D. Gogny, Hartree-Fock-Bogolyubov calculations with the D1 effective interaction on spherical nuclei, *Phys. Rev. C* **21**, 1568 (1980).
- [43] D. Gogny, Self-consistent pairing calculations (North-Holland Publishing Company, 1975).
- [44] D. Gogny, Proceedings of the international conference on nuclear physics, Munich, august 27-september 1, p.48 (1973).
- [45] N. Dubray *et al.*, in preparation.
- [46] C. Wagemans, E. Allaert, A. Deruytter, R. Barthélémy, and P. Schillebeeckx, Comparison of the energy and mass characteristics of the $^{239}\text{Pu}(\text{nth},\text{f})$ and the $^{240}\text{Pu}(\text{sf})$ fragments, *Phys. Rev. C* **30**, 218, (1984).
- [47] P. Schillebeeckx, C. Wagemans, A. J. Deruytter, and R. Barthélémy, Comparative study of the fragments' mass and energy characteristics in the spontaneous fission of ^{238}Pu , ^{240}Pu and ^{242}Pu and in the thermal-neutron-induced fission of ^{239}Pu , *Nucl. Phys. A* **545**, 623 (1992).
- [48] K. Nishio, Y. Nakagome, I. Kanno, and I. Kimura, Measurement of Fragment Mass Dependent Kinetic Energy and Neutron Multiplicity for Thermal Neutron Induced Fission of Plutonium-239, *J. Nucl. Sci. Technol.* **32**, 404 (1995).
- [49] C. Tsuchiya, Y. Nakagome, H. Yamana, H. Moriyama, K. Nishio, I. Kanno, K. Shin, and I. Kimura, Simultaneous Measurement of Prompt Neutrons and Fission Fragments for $^{239}\text{Pu}(\text{nth},\text{f})$, *J. Nucl. Sci. Technol.* **37**, 941 (2000).
- [50] W. Reisdorf, J. P. Unik, H. C. Griffin, and L. E. Glendenin, Fission fragment K x-ray emission and nuclear charge distribution for thermal neutron fission of ^{233}U , ^{235}U , ^{239}Pu and spontaneous fission of ^{252}Cf , *Nucl. Phys. A* **177**, 337 (1971).
- [51] N. Boucheneb, M. Asghar, G. Barreau, T. P. Doan, B. Leroux, A. Sicre, P. Geltenbort, and A. Oed, A high-resolution multi-parametric study of $^{239}\text{Pu}(\text{nth},\text{f})$ with the Cose-Fan-Tutte spectrometer, *Nucl. Phys. A* **535**, 77 (1991).
- [52] C. Simenel, Particle Transfer Reactions with the Time-Dependent Hartree-Fock Theory Using a Particle Number Projection Technique, *Phys. Rev. Lett.* **105**, 192701 (2010).
- [53] M. Verriere, N. Schunck, and D. Regnier, Microscopic calculation of fission product yields with particle-number projection, *Phys. Rev. C* **103**, 054602 (2021).
- [54] W. Von Oertzen, Martin Freer, Yoshiko Kanada-En'yo, Nuclear clusters and nuclear molecules, *Phys. Rep.* **432**, 43 (2006).
- [55] M. Warda and L. M. Robledo, Microscopic description of cluster radioactivity in actinide nuclei, *Phys. Rev. C* **84**, 044608 (2011).
- [56] M. Girod and P. Schuck, Alpha-Particle Clustering from Expanding Self-Conjugate Nuclei within the Hartree-Fock-Bogoliubov Approach, *Phys. Rev. Lett.* **111**, 132503 (2013).
- [57] A. Zdeb, M. Warda, and K. Pomorski, Half-lives for α and cluster radioactivity within a Gamow-like model, *Phys. Rev. C* **87**, 024308 (2013).
- [58] M. Warda, A. Zdeb, and L. M. Robledo, Cluster radioactivity in superheavy nuclei, *Phys. Rev. C* **98**, 041602 (2018).
- [59] J.-P. Ebran, M. Girod, E. Khan, R. D. Lasserri, and P. Schuck, α -particle condensation: A nuclear quantum phase transition, *Phys. Rev. C* **102**, 014305 (2020).
- [60] F. Mercier, J. Zhao, J.-P. Ebran, E. Khan, T. Nikšić, and D. Vretenar, Microscopic Description of 2α Decay in ^{212}Po and ^{224}Ra Isotopes, *Phys. Rev. Lett.* **127**, 012501 (2021).